

## Intensity of the Soft and Hard Component of the Cosmic Radiation as a Function of Altitude at Geomagnetic Latitudes of 28°N, 41°N, and 55°N\*

MARCELLO L. VIDALET†

Department of Physics, University of Chicago, Chicago, Illinois

(Received August 6, 1951)

Counter telescopes have been flown with plastic balloons to a maximum altitude of 94,000 ft. Intensity *vs* pressure curves have been obtained at geomagnetic latitudes of  $\lambda=55^\circ$ ,  $41^\circ$ , and  $28^\circ$  for the total cosmic radiation and for the components capable of traversing several thicknesses of lead. The energy spectrum of primary cosmic-ray particles has been derived from the extrapolation of the intensity of the total radiation to the top of the atmosphere. The integral momentum spectrum of the total primary radiation is given by  $N(>pc/Ze)=0.49(pc/Ze)^{-1.0}$ . The results show that the radiation originating from primaries in the energy range 1 to 4 Bev (cut-off energies at  $\lambda=55^\circ$  and  $41^\circ$ ) is predominantly of a nucleonic nature. The absence of an appreciable electronic component can be explained by assuming that,

close to the top of the atmosphere, electrons originate predominantly from the decay of neutral mesons and that, within this energy range, the over-all probability of nucleon emission is greater than that of meson production. In sharp contrast, the soft component originating from primaries in the range from 4 to 8 Bev (cut-off at  $\lambda=41^\circ$  and  $28^\circ$ ) multiplies rapidly in the atmosphere. This large transition effect in air with a maximum at about 10 cm Hg pressure is very characteristic of electron showers. It is concluded that the probability of neutral mesons being produced is comparatively high at primary energies between 4 and 8 Bev. At energies higher than 8 Bev this effect is even more pronounced, due to the contribution of the plural and multiple production of mesons.

### I. INTRODUCTION

SEVERAL experiments have been performed in an attempt to gain a better understanding of nuclear events leading to the production of mesons and secondary nucleons. Since different types of particles are in general absorbed in matter with a different mean free path, it can be expected that a study of the intensity of the cosmic radiation as a function of altitude, latitude, and penetrability in lead will provide information regarding the nature of the various cosmic-ray components.

Millikan and his collaborators<sup>1</sup> have made extensive measurements of the total intensity of the cosmic radiation in a series of balloon flights at various latitudes. The hard component has been studied by Schein and collaborators<sup>2</sup> in a number of investigations using

counter telescopes with lead absorbers of several thicknesses interposed between the counters. Experiments of a similar nature have been performed by other workers<sup>3-7</sup> during the past few years. In view of many recent improvements in balloon techniques which permit the study of the cosmic radiation up to a pressure equivalent to less than 15 g/cm<sup>2</sup> of air, it was considered advisable to conduct a further series of flights using counter telescopes of similar geometry so as to obtain results which are directly comparable. In these flights the total, soft, and hard components were measured simultaneously using a technique previously reported by M. Schein at the Pasadena Conference of Cosmic Radiation.<sup>8</sup> This technique permits the comparison of the various components of the cosmic radiation under identical atmospheric conditions. Furthermore, time variations in the intensity of the cosmic radiation due to solar activity and other sources can be recognized by the fact that the variations are not the same for the various components.

### II. BALLOON FLIGHT TECHNIQUES

The apparatus, consisting of the counters, coincidence circuits, power packs, and recording unit was mounted inside a light Dow-metal frame covered with pyraline, a transparent plastic very opaque to infrared radiation. Bands of aluminum foil around the gondola reflected the proper amount of solar radiation to maintain the equipment close to room temperature. During the flight a record was kept of the temperature inside the gondola, which showed that in most cases the temperature averaged 20°C.

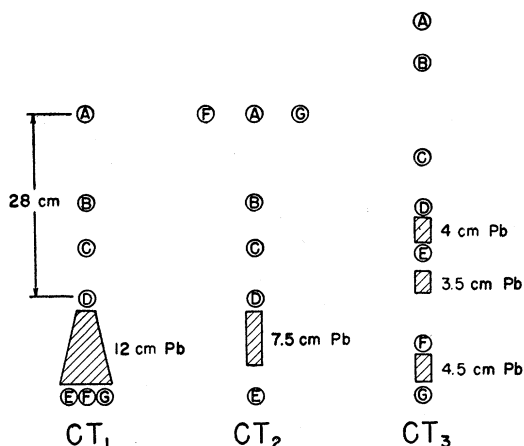


FIG. 1. Counter telescopes used for the measurement of the intensity of the cosmic-ray components.

\* Assisted by the joint program of the ONR and AEC.

† Now at Princeton University, Princeton, New Jersey.

<sup>1</sup> Millikan, Neher, and Pickering, Phys. Rev. **61**, 396 (1942).

<sup>2</sup> Schein, Jesse, and Wollan, Phys. Rev. **59**, 615 (1941).

<sup>3</sup> M. Pomerantz, Phys. Rev. **75**, 69 (1949).

<sup>4</sup> Winckler, Stix, Dwight, and Sabin, Phys. Rev. **79**, 656 (1950).

<sup>5</sup> M. Vidale and M. Schein, Phys. Rev. **81**, 1065 (1951); Nuovo cimento **VIII**, 10 (1951).

<sup>6</sup> Rao, Balasubrahmanyam, Gokhale, and Pereira, Phys. Rev. **83**, 173 (1951).

<sup>7</sup> J. D. Pullar and E. G. Dymond, Phil. Mag. **42**, 663 (1951).

<sup>8</sup> See J. R. Oppenheimer, Revs. Modern Phys. **21**, 181 (1949).

TABLE I. Summary of flight data.

Flight number	Type of equipment	Date	Geom. lat.	Duration of flight (hours)	Rate of ascent (ft/min)	Maximum cm Hg pressure	Altitude ft
I	Counter telescope $CT_1$	Nov. 15, 1949	28°	8 $\frac{3}{4}$	670	1.1	94,000
II	Counter telescope $CT_1$	June 6, 1950	55°	10 $\frac{1}{2}$	330 to 60,000 ft 160 above 60,000 ft	1.6	86,000
III	Counter telescope $CT_2$	Aug. 4, 1950	55°	8 $\frac{1}{2}$	710	1.2	93,000
IV	Counter telescope $CT_3$	Jan. 13, 1951	41°	6	120	4.0	66,000
V	Counter telescope $CT_3$	Feb. 4, 1951	41°	6 $\frac{1}{2}$	450	1.7	84,000

Each apparatus was tested inside a large tank which was evacuated down to a pressure of 0.5 cm Hg, a pressure lower than the lowest pressure reached in any of the balloon flights. This was done in order to check the performance of the circuits under conditions similar to those found in the stratosphere and, in particular, to guarantee that corona discharges could not occur across the high voltages required for the operation of the Geiger counters.

The counter equipment used in these investigations was flown with plastic, constant level balloons manufactured by the General Mills Company. The cosmic-ray equipment was released from the balloon at a predetermined time and dropped to the ground by parachute. The apparatus was promptly recovered in every case. The essential characteristics of each flight are summarized in Table I.

In every flight, pressure readings were obtained by two or more independent methods. The pressure device consisted of the following:

- (1) Barograph with temperature-compensated elements.
- (2) Radiosonde or Olland cycle type barometer which transmitted pressure data to the ground station.
- (3) In flights IV and V (see Table I) two mercury  $U$ -tubes were photographed at 10-minute intervals. The  $U$ -tubes gave very accurate ( $\sim 0.3$  mm Hg) altitude data for pressures lower than 12 cm Hg.

### III. DESCRIPTION OF THE APPARATUS

The counter telescopes used for the measurement of the vertical intensity of the cosmic radiation are shown in Fig. 1. Each apparatus contained several vertical telescopes of Geiger-Müller counters arranged to detect fourfold coincidences.  $CT_1$  and  $CT_2$  (see Fig. 1) recorded coincidences of the type  $ABCD$ ,  $BCDE$ ,  $BCDF$ , and  $BCDG$ , and  $CT_3$  recorded coincidences  $ABCD$ ,  $BCDE$ ,  $CDEF$ , and  $DEFG$ .

All Geiger-Müller counters were 2.4 cm in diameter and had an active length of 12.5 cm. The distance between the centers of the two extreme counters in each of the fourfold vertical telescopes was the same and amounted to 28 cm. Assuming that all particles are incident on the equipment isotropically, the correction to be applied to the measured vertical cosmic-ray intensity due to the finite dimensions of the counter

telescopes can be shown to amount to less than 2 percent. The effect on solid angle calculations of particles giving rise to secondaries in the lead blocks interposed between the counters will be discussed in Sec. VI. The wall thickness of the brass counters used was 0.08 cm. Hence, in order to produce a fourfold coincidence, an incident particle, depending on its direction, had to penetrate a minimum of 5 to 7 g/cm<sup>2</sup> of brass.

Each fourfold coincidence caused the flash of a neon bulb which was separately recorded as a narrow line on a photographic film. Corrections arising from the finite resolving time of the recorder are quite negligible except in the measurement of the intensity of the total component at high latitude; however, they are taken into account for all cases.

The length of the coincidence pulses of the circuits used in the equipment was 20 microseconds. Due to the fact that only fourfold coincidences were recorded, the number of accidentals was reduced to a negligible fraction of the counting rate of the telescopes. The dead time of the counters following each discharge was determined in the laboratory under conditions similar to those found in the stratosphere by placing a radium source at a certain distance from the counters. The dead time reduces the fourfold counting rate by 5 percent at a single counter counting rate of 60 counts/sec.

The individual counter telescopes were accurately tested on the ground before each balloon flight. Since the telescopes which were designed to have the same

TABLE II. Counting rate of telescopes at  $\lambda = 55^\circ$ .

Pressure (cm Hg)	55° geomagnetic latitude				
	0 cm Pb absorber (counts/min)	Pressure (cm Hg)	7.5 cm Pb absorber (counts/min)	Pressure (cm Hg)	12 cm Pb absorber (counts/min)
1.2	20.7 ± 0.2	1.2	12.0 ± 0.2	1.6	10.3 ± 0.3
2.5	22.2 ± 0.5	2.7	12.8 ± 0.7	2.2	10.1 ± 0.3
3.8	24.4 ± 0.8	7.4	10.7 ± 0.6	3.4	10.6 ± 0.5
5.0	26.2 ± 1.0	17.0	4.8 ± 0.6	4.8	10.7 ± 0.7
6.5	25.7 ± 1.0	28.0	2.4 ± 0.8	5.8	9.9 ± 0.8
8.5	22.2 ± 0.8	76.0	0.57 ± 0.02	7.5	9.1 ± 1.0
11.0	21.3 ± 0.9			9.5	8.4 ± 0.7
14.6	16.7 ± 0.9			12.2	6.9 ± 0.7
20.8	13.1 ± 0.8			16.2	5.2 ± 0.7
28.2	6.4 ± 0.5			21.8	2.7 ± 0.5
36.0	4.3 ± 0.4			27.1	2.5 ± 0.4
76.0	0.70 ± 0.02			33.6	1.9 ± 0.4
				76.0	0.53 ± 0.02

TABLE III. Counting rate of telescopes at  $\lambda=41^\circ$  and  $28^\circ$ .

Pressure (cm Hg)	41° geomagnetic latitude				28° geomagnetic latitude		
	0 cm Pb absorber (counts/min)	4 cm Pb absorber (counts/min)	7.5 cm Pb absorber (counts/min)	12 cm Pb absorber (counts/min)	Pressure (cm Hg)	0 cm Pb absorber (counts/min)	12 cm Pb absorber (counts/min)
1.9	9.2 ±0.3	7.5 ±0.2	5.6 ±0.2	4.8 ±0.2	1.2	5.0±0.1	3.6±0.1
5.0	13.4 ±0.5	9.1 ±0.4	6.8 ±0.3	5.4 ±0.3	2.2	5.7±0.4	3.6±0.3
8.6	15.4 ±0.5	8.3 ±0.3	6.3 ±0.3	5.4 ±0.3	6.1	8.8±0.5	4.3±0.3
13.9	13.6 ±0.6	7.2 ±0.4	5.1 ±0.4	3.7 ±0.3	12.6	9.4±0.9	4.1±0.6
20.6	11.1 ±0.4	5.3 ±0.3	3.6 ±0.2	3.3 ±0.2	17.3	6.0±0.5	3.8±0.5
23.0	8.2 ±0.6	4.6 ±0.5	3.5 ±0.5	2.5 ±0.4	25.0	5.6±0.6	2.1±0.4
38.0	3.2 ±0.2	2.3 ±0.2	1.8 ±0.2	1.8 ±0.2	35.0	2.3±0.5	1.5±0.3
65.3	0.88±0.03	0.79±0.03	0.66±0.03	0.62±0.03			

geometry gave the same counting rate within a statistical error of 3 percent, it has to be concluded that the individual counters were lined up correctly within the precision of the experiment. Tests were also made to guarantee that the lead blocks covered completely the active area of the counters.

#### IV. EXPERIMENTAL RESULTS

In a series of balloon flights (see Table I) at  $\lambda=55^\circ$ ,  $41^\circ$ , and  $28^\circ$  N, the intensity of the various cosmic-ray components was measured as a function of altitude using counter telescopes with varying amounts of lead interposed between the counters. In most of the flights the rate of rise of the balloon was sufficiently low to

give statistically significant data for the dependence of cosmic-ray intensity on altitude. As a consequence, these series of flights had considerable advantages over those of previous investigators in studying cosmic-ray components of low intensity and in considering differences between counting rates of various components at one particular altitude.

Tables II and III give the counting rate of the four-fold coincidences<sup>9</sup> in telescopes  $CT_1$ ,  $CT_2$ , and  $CT_3$  (see Fig. 1) at  $\lambda=55^\circ$ ,  $41^\circ$ , and  $28^\circ$ . Each value has been corrected for accidental coincidences, dead time losses, and losses due to the resolving time of the recording unit as discussed in Sec. III. The error given for each experimental point represents the standard statistical error obtained from the square root of the number of counts in the individual telescopes.

Curves  $T_{55}$ ,  $T_{41}$ , and  $T_{28}$  in Figs. 2, 3, and 4 are plots of the total vertical intensity of the cosmic radiation at the three latitudes of  $\lambda=55^\circ$ ,  $41^\circ$ , and  $28^\circ$ , respectively. For comparison these curves are presented together in Fig. 5. All three curves show a pronounced maximum which occurs at an increasing altitude at higher latitudes.

Curves  $H_{55}$ ,  $H_{41}$ , and  $H_{28}$  in Figs. 2, 3, and 4 represent the vertical intensity of the penetrating component of the cosmic radiation capable of traversing 12 cm of lead. For comparison these three curves are given in Fig. 6. It can be seen that the intensity of the penetrating component increases up to a pressure of 5, 7, and 9 cm Hg at  $\lambda=55^\circ$ ,  $41^\circ$ , and  $28^\circ$ , respectively. At these pressures the three curves show relatively flat maxima.

The vertical intensity through 4 and 7.5 cm of lead was measured in order to obtain intermediate points between the total and the hard component. The intensity of the cosmic radiation through 4 cm of lead was obtained at  $\lambda=41^\circ$  (curve  $I_{41}$  in Fig. 3) and through 7.5 cm of lead at  $\lambda=55^\circ$  and  $41^\circ$  (curves  $J_{55}$  and  $J_{41}$  in Figs. 2 and 3).

The intensity vs altitude curves obtained at  $\lambda=55^\circ$  (Fig. 2) do not extrapolate to a common point at the top of the atmosphere. At  $\lambda=41^\circ$  and  $28^\circ$  (Figs. 3 and 4) a similar effect seems to exist; however, it is less pro-

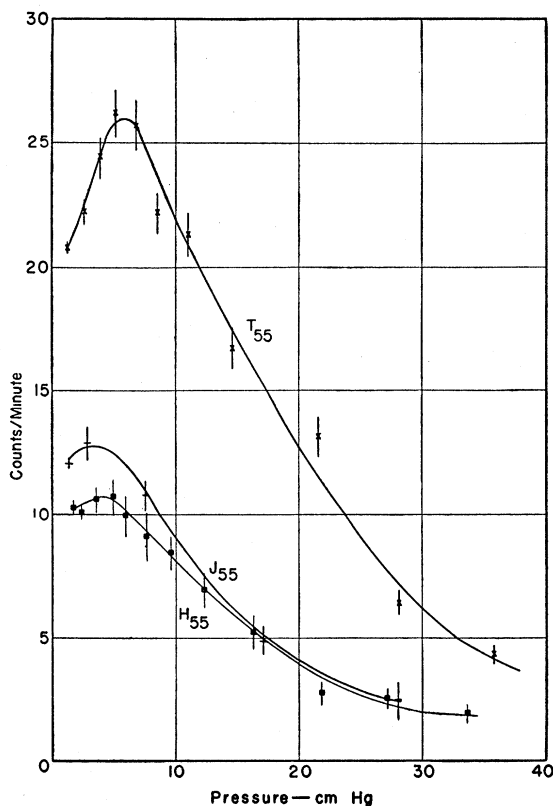


FIG. 2. Altitude dependence of the intensity of the cosmic radiation at  $\lambda=55^\circ$  as measured through 0 cm of lead ( $T_{55}$ ), 7.5 cm of lead ( $J_{55}$ ), and 12 cm of lead ( $H_{55}$ ).

<sup>9</sup> Re-evaluation of the pressure data in flight II at  $\lambda=55^\circ$  has indicated a small discrepancy in the time vs altitude curve between 0 and 45,000 ft. (This change results in a shift toward higher pressures of the intensity measurements reported in reference 5.)

nounced because of the better collimation of penetrating secondaries in the forward direction due to the considerably higher cut-off energy of the primary radiation. At  $\lambda=55^\circ$  the difference in the extrapolated intensity of the total and the hard component through 12 cm of lead amounts to approximately 50 percent, as compared to about 30 percent at  $\lambda=41^\circ$  and to about 15 percent at  $\lambda=28^\circ$ . This effect can be understood by noting that primary cosmic-ray particles incident on the equipment at these latitudes interact with nuclei of the lead absorber. These interactions, which are known to occur with a collision cross section approximately equal to the geometrical area of the lead nucleus, lead to the emission of secondary particles which in turn can be absorbed or scattered out of the counter telescope. At low latitudes, where the primary particles have a higher average energy, this effect is considerably smaller, as secondary particles which are produced in 12 cm of lead and which are emitted forward have often sufficient energy to traverse the remaining amount of lead and trigger the lower counter of the telescope. The effect of the presence of the lead absorber on the geometry of the counter telescope will be discussed in Sec. VI.

The latitude effect (intensity at  $\lambda=55^\circ$  or  $41^\circ$ /intensity at  $\lambda=28^\circ$ ) of the total and hard components of the cosmic radiation at  $\lambda=55^\circ$  and  $41^\circ$  is given in Table IV for a few selected altitudes in the atmosphere. One can see that at all altitudes the total radiation shows a larger latitude effect than the hard component. For both components, the latitude effect reaches its highest value at the top of the atmosphere.

From Figs. 2, 3, and 4 one can obtain the difference curves representing the contribution to the intensity of the cosmic radiation of primaries in the energy range 1 to 4 Bev (cut-off energy from the vertical at  $\lambda=55^\circ$  and  $41^\circ$ ), 4 to 8 Bev (cut-off at  $\lambda=51^\circ$  and  $28^\circ$ ) and  $>8$  Bev (cut-off at  $\lambda=28^\circ$ ). Curves  $H_{55-41}$  and  $S_{55-41}$  in Fig. 7 represent, respectively, the intensity of the penetrating radiation and of the radiation absorbed in 12 cm of lead originating from primaries in the energy range 1 to 4 Bev. From the absorption of these two components in air, it appears that electrons cannot be present in large numbers, as they would produce a strong transition effect close to the top of the atmosphere and would not contribute to the penetrating component.  $\mu$ -mesons would be absorbed in air less rapidly than indicated by  $H_{55-41}$ . Hence, it is concluded that primary and secondary nucleons are mainly responsible for the two components represented by these curves.

Curves  $H_{41-28}$  and  $S_{41-28}$  in Fig. 7 represent the penetrating component and the component absorbed in 12 cm of lead originating from primaries in the energy range between 4 and 8 Bev. The large increase by a factor of 2 in the intensity of the soft component between the atmospheric pressure of 1.5 and 12 cm Hg is strong evidence that primaries in the energy range 4 to 8 Bev give rise to electronic cascades in the atmosphere. This effect can be explained by assuming

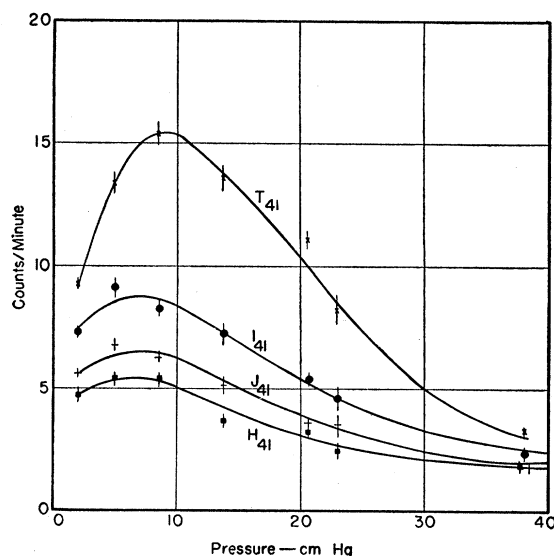


Fig. 3. Altitude dependence of the intensity of the cosmic radiation at  $\lambda=41^\circ$  as measured through 0 cm of lead ( $T_{41}$ ), 4 cm of lead ( $I_{41}$ ), 7.5 cm of lead ( $J_{41}$ ), and 12 cm of lead ( $H_{41}$ ).

that, as the result of the decay of neutral mesons into two  $\gamma$ -rays, electron showers of moderate multiplicity are initiated in air.<sup>10</sup> The very low intensity of the penetrating component is apparently due to the fact that charged  $\pi$ -mesons produced in the primary interaction decay into  $\mu$ -mesons with a short mean life and hence do not give rise to subsequent nucleonic cascades.

Curves  $H_{28}$  and  $S_{28}$  in Fig. 7 represent, respectively, the penetrating component and the component stopped in 12 cm of lead originating from primaries of energy greater than 8 Bev. Both components show a marked transition effect with a maximum intensity at approximately 9 cm Hg pressure. From 1.5 to 9 cm Hg pressure the soft component increases by a factor of 3.2 and the hard component by 1.2. This strong multiplication in

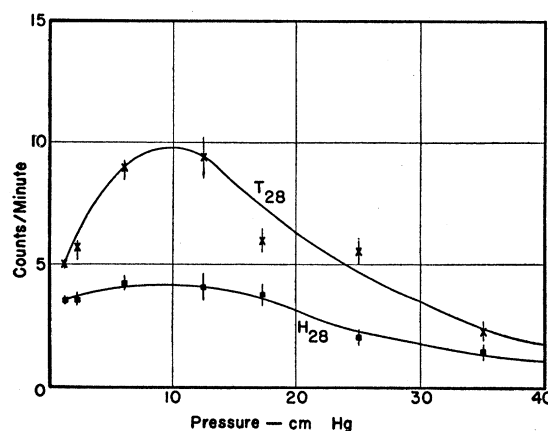


Fig. 4. Altitude dependence of the intensity of the cosmic radiation at  $\lambda=28^\circ$  as measured through 0 cm of lead ( $T_{28}$ ) and 12 cm of lead ( $H_{28}$ ).

<sup>10</sup> B. Rossi, *Revs. Modern Phys.* 21, 104 (1949).

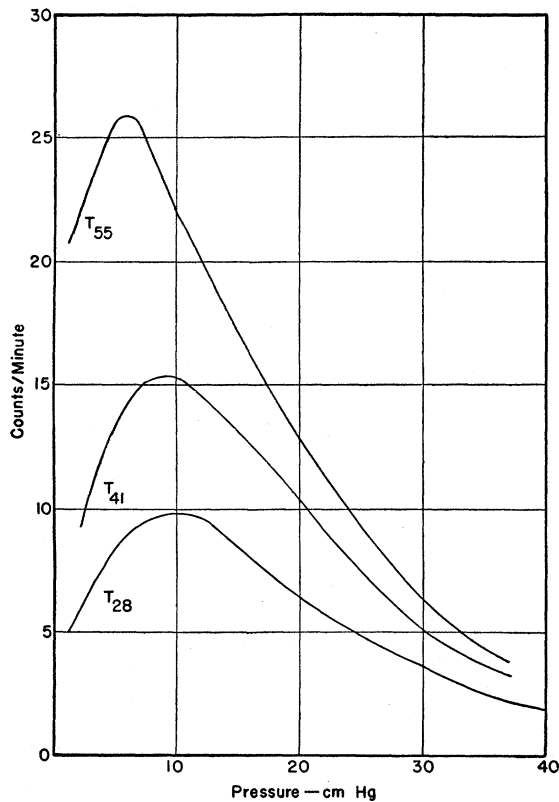


FIG. 5. Altitude dependence of the total vertical cosmic radiation at  $\lambda=55^\circ$  ( $T_{55}$ ),  $\lambda=41^\circ$  ( $T_{41}$ ), and  $\lambda=28^\circ$  ( $T_{28}$ ).

the first few mean free paths in the atmosphere indicates that primaries having an energy greater than 8 Bev can produce, in their interactions with air nuclei, nucleonic cascades of higher multiplicity. The fact that the soft and hard components reach their maximum intensity at approximately the same atmospheric depth is an added indication that both must have a common origin, namely, those nuclear interactions which give rise to neutral and charged mesons.

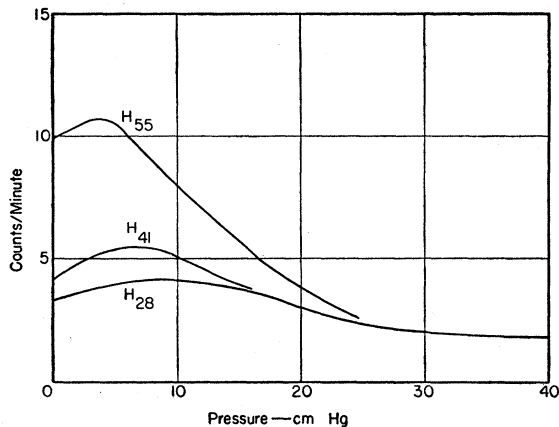


FIG. 6. Altitude dependence of the hard component of the cosmic radiation as measured through 12 cm of lead at  $\lambda=55^\circ$  ( $H_{55}$ ),  $\lambda=41^\circ$  ( $H_{41}$ ), and  $\lambda=28^\circ$  ( $H_{28}$ ).

Figure 8 gives the absorption of the radiation in lead at  $\lambda=41^\circ$  for atmospheric pressures of 8, 2, and 0 cm Hg (curves A, B and C, respectively). The primary cosmic radiation (obtained by extrapolating curves  $T_{41}$ ,  $I_{41}$ ,  $J_{41}$ , and  $H_{41}$  to the top of the atmosphere, see Fig. 3) is absorbed in lead with a mean free path of 300 g/cm<sup>2</sup>, approximately. From these results the following conclusions can be drawn:

(a) The number of primary and secondary electrons present at the top of the atmosphere is negligible (less than a few percent) since they would show a rapid absorption in lead, which is clearly not the case.

(b) The value obtained for the absorption mean free path of the primary radiation is approximately two times the geometrical mean free path of protons and is in good agreement with results of other investigators<sup>11</sup> on the absorption of high energy nucleons in lead at lower altitudes. An admixture of 10–15 percent alpha-particles is consistent with the shape of the absorption curve in Fig. 8.

(c) The contribution of particles originating within the apparatus and of low energy albedo nucleons from the lower atmosphere must be small since their presence

TABLE IV. Latitude effect of the total and hard components.

Pressure (cm Hg)	55° geomagnetic latitude		41° geomagnetic latitude	
	Total	Hard	Total	Hard
0.0	4.9	3.0	1.7	1.3
1.2	4.2	3.0	1.7	1.3
6.0	2.9	2.5	1.6	1.3
10.0	2.2	1.9	1.5	1.2

in appreciable numbers would tend to make the absorption curve considerably steeper.

At an atmospheric pressure of 8 cm Hg (corresponding to the maximum intensity of the total radiation at  $\lambda=41^\circ$ ), the large drop in the absorption curve of Fig. 8 between 0 and 4 cm of lead is typical for electrons and hence clearly shows the presence of an abundant electronic component ( $\sim 30$  percent) at these lower altitudes (50,000 ft).

#### V. INTENSITY OF THE PRIMARY RADIATION

The magnetic field of the earth determines,<sup>12,13</sup> as a function of latitude, the minimum energy that cosmic-ray particles must have in order to enter the atmosphere from outer space. This cut-off energy for particles incident from the vertical direction at  $\lambda=55^\circ$ ,  $41^\circ$ , and  $28^\circ$  is given in Table V.

The vertical flux of the radiation (number of particles/cm<sup>2</sup> sterad sec) traversing a counter telescope can be obtained by multiplying the observed counting rate (counts/sec) by a factor  $f$  which is calculated from the known geometry of the telescope. In the present

<sup>11</sup> T. A. Stinchcomb, Phys. Rev. **83**, 422 (1951).

<sup>12</sup> M. S. Vallarta, Phys. Rev. **74**, 1837 (1948).

<sup>13</sup> R. A. Alpher, J. Geophys. Res. **55**, 437 (1950).

case, a standard telescope subtends a solid angle  $\propto$  area  $f=1.06$  cm<sup>2</sup>-sterad for isotropic distribution of the incident radiation. Table VI gives the flux of the primary radiation incident on the atmosphere at  $\lambda=55^\circ$ ,  $41^\circ$ , and  $28^\circ$  as extrapolated from curves  $T_{55}$ ,  $T_{41}$ , and  $T_{28}$  (Fig. 5) of the total radiation to the top of the atmosphere after subtraction of those events due to showers originating within the equipment (see Sec. VI).

The total primary flux can be approximated by an integral power spectrum of the following type:

$$N(>pc/Ze) = (0.49 \pm 0.04)(pc/Ze)^{-1.0 \pm 0.1}.$$

Recent measurements of the total cosmic radiation made above the atmosphere in experiments carried out in rockets<sup>14</sup> give a spectrum in substantial agreement with the one obtained here, though the absolute intensity is 20 percent less than here. This difference may be due to the different geometry of the telescopes and to the different disposition of the heavy material in the apparatus. It may be noted that in rocket experiments events which were due to showers originating in the equipment and were subtracted from the total counting rate in the estimate of the total primary

TABLE V. Geomagnetic cut-off of primary cosmic-ray particles incident from the vertical direction.

Geom. lat.	Protons Energy (Bev)	Heavy nuclei ( $Z \geq 2$ ) Energy per nucleon
$55^\circ$	1.0	0.35
$41^\circ$	4.0	1.5
$28^\circ$	8.1	3.5

flux represent a contribution several times larger than in the present work.

The primary spectrum can also be compared with the results obtained by Winckler *et al.*<sup>4</sup> using telescopes with 3 cm of lead interposed between the counter trays. However, due to the absorption in lead of a fraction of the radiation of lower energy, the results indicate that the flux given by Winckler at  $55^\circ$  is 15 percent lower than the flux found with counter telescopes without lead absorber.

#### VI. EFFECT OF SHOWERS, SCATTERING, AND GEOMETRY OF TELESCOPES

In the determination of the intensity of the cosmic radiation by means of counters, the effect of local and air showers has to be considered. In order to reduce the number of showers originating in the equipment that might discharge the coincidence arrangements, no heavy material was placed alongside or above the counters. The importance of this effect can be estimated from the number of coincidences  $FBCD$  and  $GBCD$  detected in equipment  $CT_2$  (see Fig. 1) at  $\lambda=55^\circ$ , where the highest out-of-line counting rate was found to be

<sup>14</sup>J. A. Van Allen and S. F. Singer, Phys. Rev. 78, 819 (1950).

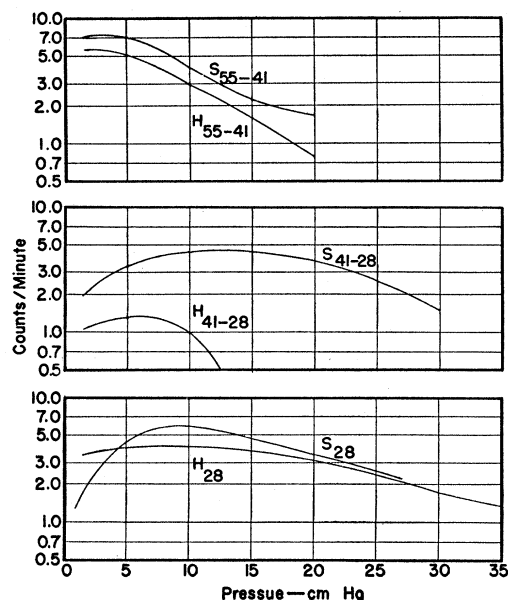


FIG. 7. Altitude dependence of the intensity of the penetrating radiation ( $H$ ) and of the radiation absorbed in 12 cm of lead ( $S$ ) originating from primaries in the energy range: 1 to 4 Bev (cut-off energy at  $\lambda=55^\circ$  and  $41^\circ$ ), 4 to 8 Bev ( $\lambda=41^\circ$  and  $28^\circ$ ) and  $>8$  Bev ( $\lambda=28^\circ$ ).

7 percent of the corresponding rate for counters  $ABCD$ . Other investigators with similar counter arrangements have obtained values of the same magnitude.<sup>15,16</sup>

The location of the lead in the counter train affects the geometry of the counter telescope due to the interactions of incident particles within the absorber. These types of interactions were studied with apparatus  $CT_1$  at  $\lambda=55^\circ$  and  $28^\circ$ . Let  $I$  be the extrapolated flux (number of particles per cm<sup>2</sup> per sterad per sec) of the cosmic radiation incident on telescope  $BCDF$  ( $f=1.06$

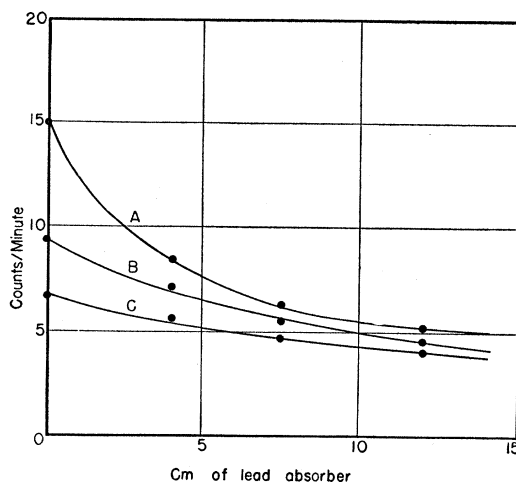


FIG. 8. Absorption of the cosmic radiation in lead at  $\lambda=41^\circ$  measured at an atmospheric pressure of: A, 8 cm Hg; B, 2 cm Hg; C, 0 cm Hg.

<sup>15</sup>T. H. Johnson and J. G. Barry, Phys. Rev. 57, 245 (1940).

<sup>16</sup>Schein, Wollan, and Groetzinger, Phys. Rev. 58, 1027 (1940).

TABLE VI. Primary flux of the cosmic radiation.

Geomagnetic latitude	55°	41°	28°
Total primary flux (per cm <sup>2</sup> sterad sec)	0.296±0.02	0.102±0.01	0.059±0.01

cm<sup>2</sup>-sterad) at the top of the atmosphere as determined in Sec. V. The counting rate under 12 cm of lead (132 g/cm<sup>2</sup>) at 0 cm Hg pressure is due to the following:

(a) primary particles, assumed to be all protons, that traverse the lead absorber without undergoing nuclear collisions,

(b) primary particles incident within the solid angle  $\times$  area defined by counters *BCDF* which interact in the absorber and give rise to secondaries detected by counter *F* below the lead,

(c) primary particles incident within a solid angle not included by counters *BCDF*, but which traverse counters *BCD*. These particles may interact in the lead absorber and, through the action of secondary particles, register a quadruple coincidence *BCDF*. A graphical integration of their path length in lead gives, for events of this type, an effective solid angle  $\times$  area  $f' = 2.33$  cm<sup>2</sup>-sterad.

At the top of the atmosphere the counting rate of telescope *BCDF* will be given therefore by the following expression:

$$F = 1.06Ie^{-132/\lambda_{\text{Pb}}} + (1.06a + 2.33a')I(1 - e^{-132/\lambda_{\text{Pb}}}),$$

where  $\lambda_{\text{Pb}}$  (g/cm<sup>2</sup>) is the collision mean free path of protons in lead and  $a$  and  $a'$  are constants giving the probability that after collision one or more of the secondary particles traverse the bottom counter of the telescope.

The solid angle subtended by counters *BCDE* and *NCDE* (see Fig. 1) was half as wide as that of telescope *BCDF*. This was determined geometrically from the location of the counters and also from their respective ground counting rate. Since at sea level penetrating particles consist mainly of  $\mu$ -mesons which do not interact appreciably in matter, the counting rate observed, neglecting the small effect of zenith angle dependence, is directly proportional to the solid angle defined by the telescope. It follows that the counting rate of *BCDE* and *BCDG* above the atmosphere is given approximately by the following expression:

$$G = \frac{1}{2}(1.06)Ie^{-132/\lambda_{\text{Pb}}} + (1.06a + 2.33a')I(1 - e^{-132/\lambda_{\text{Pb}}}).$$

The intensity of the extrapolated primary flux  $I$  is given in Sec. V and the counting rates of telescopes *BCDF*, *BCDE*, and *BCDG* were obtained in flights I and II (see Table I). Since the collision mean free path  $\lambda_{\text{Pb}}$  is 160 g/cm<sup>2</sup>, one finds:

$$\begin{aligned} F_{55} &= 0.137 + 0.192a_{55} + 0.420a'_{55} = 0.163 \text{ counts/sec;} \\ G_{55} &= 0.068 + 0.192a_{55} + 0.420a'_{55} = 0.102 \text{ counts/sec;} \\ F_{28} &= 0.027 + 0.038a_{28} + 0.083a'_{28} = 0.055 \text{ counts/sec;} \\ G_{28} &= 0.014 + 0.038a_{28} + 0.083a'_{28} = 0.035 \text{ counts/sec.} \end{aligned}$$

Since secondary particles of high energy are known<sup>17</sup> to be collimated in the direction opposite to the incoming particle, it will be assumed that  $a' = a/2$ . From the above equations one can solve for two independent values of  $a$  at each latitude. Their average value is very approximately  $a_{55} = 0.075$  and  $a_{28} = 0.31$ .

These results indicate that particles incident on the equipment from outside the solid angle defined by counters *BCDF* (and that would be affected seriously by the geometrical disposition of the absorber) contribute roughly a maximum of 10 and 25 percent at 55° and 28° geomagnetic latitude, respectively, to the observed counting rate of the hard component. Consideration of the effect of Coulomb scattering, of knock-on electrons, and of the presence of heavy nuclei in the primary radiation would decrease the value of  $a$  in the above equations and therefore also the contribution to the hard component of particles incident within the solid angle not defined by counters *BCDF*.

Apparatus *CT*<sub>1</sub> registered the counting rate of the coincidence sets *BCDE*, *BCDF*, and *BCDG* discharged simultaneously. Such events require the tripping of all the counters below the lead block so that a minimum of three penetrating particles must be involved in the process. Since the contribution of penetrating air showers and electronic side showers is found to be negligible in such high order coincidences, events of this type must be due to penetrating events of moderate energy originating in the lead. (Coincidences between counters *ABCDGH* in equipment *CT*<sub>2</sub> at  $\lambda = 55^\circ$  occurred at the rate of 0.11 counts/min at a pressure of 1.2 cm Hg.) In flights I and II at 28° and 55°, the counting rate of counters *BCDFGE* was found to be 0.52 and 0.72 counts/min, respectively. The largest latitude effect for this kind of high energy events occurs at the highest altitude reached (1.6 cm Hg) and amounts to  $1.5 \pm 0.3$  as compared to 2.9 for the hard component and 4.1 for the total radiation.

I wish to express my sincere gratitude to Professor Marcel Schein for his guidance and encouragement during the course of this work. The cooperation of the ONR and of the staff of the General Mills Company in arranging the balloon flights and in making every effort to make these experiments successful is deeply appreciated. Thanks are due to Mr. Raymond Foster and Mr. John Bjorkland for their valuable help in the construction and operation of the equipment, and Professor G. Puppi for a very interesting discussion.

<sup>17</sup> Brown, Camerini, Fowler, Heitler, King, and Powell, *Phil. Mag.* **40**, 862 (1950).